Article

J. Mex. Chem. Soc. **2025**, *69*(1)
Special Issue

ISSN-e 2594-0317

Hydrogen Bonding Processes During Self-protonation of Natural α-hydroxyquinones

Georgina Armendáriz-Vidales,[1] Fidel Hernández-Pérez,[1] Felipe J. González-Bravo[2], Carlos Frontana*[1]

[1]Centro de Investigación y Desarrollo Tecnológico en Electroquímica, SC. Parque Tecnológico Querétaro S/N, Pedro Escobedo, Querétaro, 76703.
[2]Centro de Investigación y de Estudios Avanzados del Instituto Politécnico Nacional. Av. IPN No. 2508, Colonia San Pedro Zacatenco, Alcaldía Gustavo. A. Madero, Ciudad de México
Rafael Atlixco 186, Colonia Leyes de Reforma 1a sección, Alcaldía de Iztapalapa, Ciudad de México, 09310, México.

***Corresponding author:** Carlos Frontana, email: ultrabuho@yahoo.com.mx

Received June 1st, 2024; Accepted September 21st, 2024.

DOI: http://dx.doi.org/10.29356/jmcs.v69i1.2316

Abstract. The passage from non-substituted quinone to hydroquinone moieties involves the exchange of two-electron and two-protons, however, the presence of hydroxyl groups in the α position to the carbonyl group of the quinone induce a mechanistic change in which the quinone plays the role of electron acceptor and proton donor. This feature promotes a self-protonation mechanism which can be characterized in the framework of the ECE-DISP theory. However, when additional hydroxyl groups are contained in the quinone structure, hydrogen bonding becomes an additional competition factor that was studied in this work using a series of synthetic and natural quinones with different structures. The number of hydroxyl groups on the quinone structure was studied from the point of view of electrochemical mechanisms and descriptors of reactivity. Cyclic voltammetry, mechanistic simulation and electronic structure calculations were used as an approach to understand the interplay between electron transfer, proton transfer and hydrogen bonding association in α-hydroxyquinones.
Keywords: α-hydroquinones; self-protonation; hydrogen bonding, electroaccepting power; salicylic acid.

Resumen. La conversión quinona-hidroquinona involucra el intercambio de dos electrones y dos protones; sin embargo, la presencia de grupos hidroxilo en la posición α respecto al carbonilo de la quinona, induce un cambio mecanístico en el cual el núcleo quinoide juega ahora el papel de acceptor electrónico y donador de protón. Esta característica promueve un mecanismo de autoprotonación que puede ser caracterizado mediante la teoría ECE-DISP. Sin embargo, cuando hay grupos hidroxilo adicionales dentro de la estructura quinoide, la formación de puentes de hidrógeno se convierte en una ruta competitiva adicional, la cual fue estudiada en este trabajo empleando una serie de compuestos sintéticos y naturales. El número de grupos hidroxilo y su influencia fueron estudiados desde el punto de vista de mecanismos electroquímicos y descriptores de reactividad. A través del uso de voltamperometría cíclica, simulación mecanística y cálculos de estructura electronica, se realizó una aproximación para comprender la interrelación entre la transferencia protónica, electrónica y la asociación a través de puentes de hidrógeno en α-hidroxiquinonas.
Palabras clave: α-hidroxiquinonas; autoprotonación; puentes de hidrógeno; potencia electroaceptora; ácido salicílico.

J. Mex. Chem. Soc. **2025**, *69*(1)
Special Issue

ISSN-e 2594-0317

Introduction

Understanding the reduction processes of quinone compounds, as well as their coupled-chemical reactions, such as hydrogen bonding and proton transfer is relevant, as these compounds play an important role in the bioactive function during energy conversion in every living organism, such as cellular respiration or photosynthesis. [1-4]

An important number of quinones with biological relevance are ubiquitous in nature. In fact, medicinal plants in Mexico containing α-hydroxyquinone moieties in abietane diterpenoids (α-OHs), such as pink lapacho (*Handroanthus impetiginosus),* plumbagin (*Plumbago zeylanica),* Mexican bush sage (*Salvia leucantha*), Perezia (*Perezia adnata*), walnut tree (*Juglans regia*), henna (*Lawsonia inermis)*, among others, present interesting antipyretic, analgesic and antifungic properties, along with promising results in cancer treatment. [5] Biological reactivity of quinone-based compounds is related with the formation of Reactive Oxygen Species (ROS), which induce metabolic stress, causing alterations in biological membranes or modification in the mitochondrial electron transfer chain, leading to apoptosis. [6]

The electrochemical behaviour of the above-mentioned naturally derived α-hydroxyquinones have also been extensively investigated; furthermore, several authors concluded that their biological activity is dependent on their chemical structure, and specifically, the potential at which the radical anions are formed. [7-10] Early reports exposed their electrochemical reaction mechanisms, where the reduction taking place at the first voltametric reduction signal is significantly determined by self-protonation processes- [9,11] Regarding the stability of their electrogenerated radical anions, this issue can be nevertheless improved through stabilization by supramolecular interactions like hydrogen bonding.[12,13] Alternatively, the passage from weak to strong interactions afford intermolecular proton transfer reactions that are induced by the α-hydroxyl group. Even though such self-protonation mechanisms have been described for some naturally occurring α-OHs, in several cases, OH functionalities can also be present in nearby sites within the same molecule, which is also an important feature for their use as pharmacological moieties. Self-protonation mechanisms occur through a fractionary electronic stoichiometry (2/3), however, in the presence of an external proton source, such mechanisms change and become bielectronic. Hence, the present work was aimed towards understanding such cross-reactivity effects in a series of naturally derived α-OHs (Scheme 1) in dimethyl sulfoxide. Their overall mechanism of reduction is analyzed considering that a hydroxyl group present in the molecule at the α position can act as a proton source and the influence that nearby OH functions can have in the electrochemical mechanism. This was analysed in aprotic medium and then compared with the one obtained in the presence of an external proton donor such as salicylic acid. Finally, experimental results of some natural occurring quinones are contrasted to their reactivity indexes derived from quantum-chemical calculations.

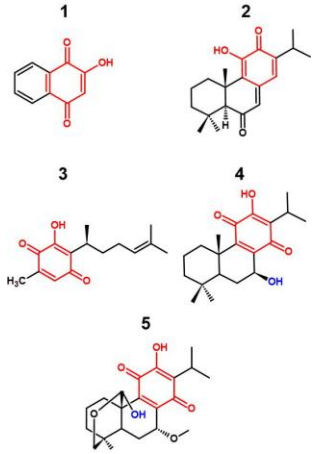

Scheme 1. Chemical structures of the α-hydroxyquinones (α-OHs): 2-hydroxy-1,4-naphthoquinone (**1**), *taxodione* (**2**), *perezone* (**3**), *horminone* (**4**) and *7α-O-methyl-conacytone* (**5**).

J. Mex. Chem. Soc. **2025**, *69*(1)
Special Issue

ISSN-e 2594-0317

Experimental section

Electrochemical experiments were performed using 1 x 10^{-3} mol L^{-1} solutions of natural α-OHs: 2-hydroxy-naphthoquinone (**1**) was purchased at Sigma-Aldrich, whereas pure samples of *taxodione* (**2**), *perezone* (**3**), *horminone* (**4**) and *7α-O-methyl-conacytone* (**5**) were obtained from natural sources. All solutions contained 0.1 mol L^{-1} tetrabutylammonium hexafluorophosphate (*n*-Bu_4NPF_6, 99 %, dried 24 h before use at 105 °C) as supporting electrolyte in dimethyl sufoxide (DMSO, 99 % extra dry over 3 Å molecular sieve). These solutions were maintained under and inert atmosphere by saturation with high-purity nitrogen (Praxair grade 5.0) for 15 minutes at room temperature (approx. 25 °C). Cyclic voltammetry experiments were carried out with an AUTOLAB PGSTAT 302N potentiostat, applying IR drop compensation by determining R_u values from positive feedback measurements until potentiostat instability was reached. A glassy carbon disk (0.0079 cm^2) was used as a working electrode, which was polished with 0.05 µm diamond powder (Buehler), sonicated and rinsed with acetone. Platinum and silver wire used as auxiliary and pseudoreference electrodes respectively. Potential values obtained were referred to the ferrocene/ferricinium (Fc/Fc^+) couple, according to the IUPAC recommendation.[14] Voltammograms were simulated employing BAS-DigiSim ver. 3.02b. Electronic structure calculations were performed with the program Gaussian 09 Revision B.01,[15] employing the density functional theory. BHandHLYP functional with a 6-311++G (2d,2p) basis set. [16,17] Optimized structures were obtained considering the solvent effect by the Marenich, Cramer and Truhlar model.[18]

Results and discussion

Electrochemical characterization of α-OHs

In order to selectively direct a chemical reaction towards the formation of a specific product, a comprehensive understanding of their reaction mechanisms is desired. For this purpose, cyclic voltammetry experiments were performed in deoxygenated dimethyl sulfoxide (DMSO). Cyclic voltammograms for solutions containing 1x10^{-3} mol L^{-1} of α-OHs, in the absence of salicylic acid are shown in Fig. 1. Under these experimental conditions, compound **1** presented two main reduction signals (Fig. 1**(A)**: Ic and IIc respectively). Ic corresponds to the formation of the corresponding hydroquinone QH_2, which is oxidized at peak Ia. In this regard, it can be pointed out that in aprotic media, a typical two-electron anodic wave is expected for hydroquinones, corresponding to an ECEC mechanism (E = electrochemical step, while C = chemical step), that is, when the radical cation is formed during the first electron transfer, it is deprotonated by the solvent itself. On the other hand, peaks IIc/IIa refer to the reversible reduction of the deprotonated quinone originated during the self-protonation mechanism occurring at the first reduction peak Ic. The reduction of these deprotonated quinone yield the radical dianion $\boldsymbol{Q^{2\bullet-}}$. [19] This self-protonation mechanism is mainly due to the higher acidity of a hydroxyl function at the α-position of the neutral quinone, which facilitates the proton removal from the first electrogenerated anion radical. [20,21]

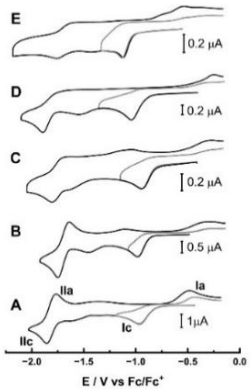

Fig. 1. Cyclic voltammograms of 1x10^{-3} mol dm^{-3} of (A) 2-hydroxy-1,4-naphthoquinone (**1**), (B) *taxodione* (**2**), (C) *perezone* (**3**), (D) *horminone* (**4**) and (E) *7α-O-methylconacytone* (**5**) on a glassy carbon electrode (A=0.0079 cm^2) in 0.1 mol L^{-1} Bu_4NPF_6 / DMSO at 0.1 Vs^{-1}.

J. Mex. Chem. Soc. **2025**, *69*(1)
Special Issue

ISSN-e 2594-0317

Table 1 shows the reduction peak potential values obtained from the voltammetric analysis of α-OHs. As shown, reduction processes of **1, 3** and **4** occurred at less negative potential values compared to **5**. Also, the reduction reaction of compound **2** occurs at a slightly more negative reduction potential, being the only notorious difference the quinone-methide nature of **2-** [22]

The difference in Ep (Ic) and Ep (Ia) values increases with the number of fused rings within the α-OHs structures.

Table 1. Data obtained from voltametric analysis of α-OHs. All the peak potential values (Ep / V) were referred to the Fc/Fc^+ couple.

Compound	Ep Ic /V	Ep Ia /V	Ep IIc /V	Ep IIa /V
1	-0.96	-0.42	-1.81	-1.72
2	-1.12	-0.53	-1.76	-1.63
3	-0.94	-0.31	-1.8	-1.68
4	-0.98	-0.23	-1.74	-1.64
5	-1.04	-0.24	-1.89	-1.69

α-OHs have been the subject of previous investigations in our group;[19,23–28] such studies showed that 2-hydroxy-1,4-naphtoquinone and *perezone* are reduced following an ECEC-DISP1 competition mechanism, whereas *horminone* is reduced through an ECEC-DISP2 mechanism.[24] It is important to remember that in the DISP1 case, the protonation of the semiquinone is the rate-determining step, whereas in the DISP2 case, protonation remains at equilibrium, and homogeneous second electron transfer is the rate determining step.

In the case of 7α-O-methyl-conacytone,[23] voltammetric analysis indicated that the ECEC-DISP1 sequence occurs, however, the experimental Ep vs log α slope is higher than that expected for this mechanism when the electron transfer is nernstian (-48.5 mV dec^{-1} *vs* theoretical -29.7 mV dec^{-1}). This result indicates the reduction process at Ic is under mixed kinetic control by the self-protonation reaction and the rate of the electron transfer. In this case, the activation electron transfer step is rather quasi reversible, such as predicted for EC mechanisms.[29] In general terms, the reduction mechanism occurring at peak Ic involves self-protonation reactions in the framework of the competition pathways depicted by the following equations:

$$\mathbf{QH + e^- \rightarrow QH^{\bullet -}} \qquad \boldsymbol{E_1^0} \qquad \text{(i)}$$

$$\mathbf{QH^{\bullet -} + QH \rightarrow QH_2^{\bullet} + Q^-} \qquad K_1 \qquad \text{(ii)}$$

$$\mathbf{QH_2^{\bullet} + e^- \rightarrow QH_2^-} \qquad E_2^{\circ}, \text{ where } E_2^{\circ} > E_1^{\circ} \qquad \text{(iii)}$$

or

$$\mathbf{QH_2^{\bullet} + QH^{\bullet -} \rightarrow QH_2^- + QH} \qquad \text{(iv)}$$

$$\mathbf{QH_2^- + QH \rightarrow QH_3 + Q^-} \qquad \text{(v)}$$

J. Mex. Chem. Soc. **2025**, *69*(1)
Special Issue

ISSN-e 2594-0317

And the overall mechanism is:

$$\mathbf{QH} + \frac{\mathbf{2}}{\mathbf{3}}\boldsymbol{e}^{-} \rightarrow \frac{\mathbf{1}}{\mathbf{3}}\mathbf{QH_3} + \frac{\mathbf{2}}{\mathbf{3}}\mathbf{Q}^{-} \qquad \text{(vi)}$$

where equations i,ii,iii and v describe the ECEC mechanism, whereas the sequence of reactions i, ii, iv and v, corresponds to a DISP mechanism.

Since the semiquinone radical anion generated during the first electron transfer is highly unstable, it self-protonates in DMSO due to the acidity of the hydroxy group at the α position within the neutral α-OH structure.[20]

As commented before,[19] the reduced species of α-OHs are prone to a series of self-protonation reactions, which can be inhibited in the presence of external protic additives. In this analysis, electrochemical behavior of α-OHs was investigated when a proton donor (AH), such as salicylic acid (pK_A=6.78 in DMSO), [30] is present. The choice of such proton donor was related to its intrinsic acidity, which is considered high enough to render any proton transfer step directly associated to the acid and not to the acidic α-hydroxy functionality.

At increasing concentrations of AH (ranging from 0.0001 to 0.1 mol L^{-1}), a noticeable change in the electrochemical behavior of compound **1** was observed where, the peak current of wave IIc diminishes whereas Ic increases (Fig. 2). At high enough concentrations of AH (higher than 0.0005 mol L^{-1}), the signal IIc disappears and peak Ic increases its current to almost three-times its original value (Fig. 2). This change agrees with the quotient of stoichiometries under self-protonation ($2/3\,e^-$, equation vi) and under assisted protonation ($2e^-$, equation xii). Under these conditions, signal Ic is associated with a direct protonation process that follows the depicted equations vii-xxii:

$$\mathrm{QH} + \mathrm{e}^- \rightarrow \mathrm{QH}^{\bullet -} \qquad E_1^\circ \qquad \text{(vii)}$$

$$\mathrm{QH}^{\bullet -} + \mathrm{AH} \rightarrow \mathrm{QH_2}^{\bullet} + A^- \qquad K_{P_1} = \frac{K_{f_1}}{K_{b_1}} \qquad \text{(viii)}$$

$$\mathrm{QH_2}^{\bullet} + \mathrm{e}^- \rightarrow \mathrm{QH_2}^- \qquad E_2^\circ \text{ where } E_2^{\circ} > E_1^{\circ} \qquad \text{(ix)}$$

or

$$^{\bullet} + \mathrm{QH}^{\bullet -} \rightarrow \mathrm{QH_2}^- + QH \qquad \text{(x)}$$

$$\mathrm{QH_2}^- + \mathrm{AH} \rightarrow \mathrm{QH_3} + A^- \qquad \text{(xi)}$$

$$\mathrm{QH} + 2\mathrm{e}^- + 2\mathrm{AH} \rightarrow \mathrm{QH_3} + 2\mathrm{A}^- \qquad \text{(xii)}$$

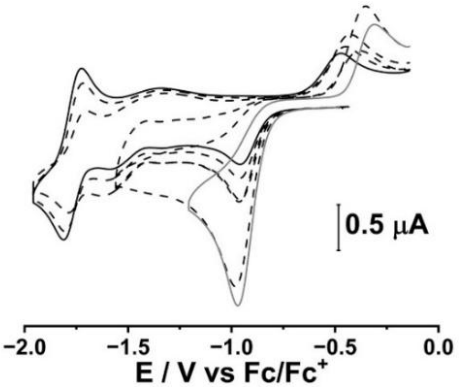

Fig. 2. Cyclic voltammetry obtained for a 1 x 10^{-3} mol L^{-1} solution of **1** in 0.1 mol L^{-1} *n*-Bu_4NPF_6 / DMSO at a sweep rate of 0.1 Vs^{-1} with increasing concentrations of salicylic acid.

J. Mex. Chem. Soc. **2025**, *69*(1)
Special Issue

ISSN-e 2594-0317

This behavior occurred for **1** – **3**, while in contrast *horminone* and *7-α-O-methyl-conacytone* (**4** and **5**) presented an extra signal (I'c, Fig. 3) that appears when the concentration of salicylic acid reaches 0.0003 mol L^{-1} and starts disappearing when concentration of AH reaches 0.0005 mol L^{-1}. It is noteworthy that upon increasing the concentration of AH, both signals transform into a single peak, I''c.

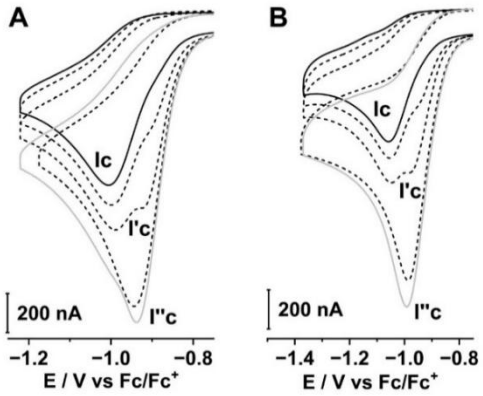

Fig. 3. Cyclic voltammetry obtained for a 1 x 10^{-3} mol L^{-1} in 0.1 M *n*-Bu_4NPF_6 / DMSO of *horminone* (**A**) and *7α-O-methyl-conacytone* (**B)** with increasing concentrations of salicylic acid [HA]. Black trace represents [HA] = 0.1 x 10^{-3} mol L^{-1}, grey trace indicates [HA] = 1.7 x 10^{-3} mol L^{-1} while the dashed lines represent intermediate concentrations.

In the case of compounds **4** and **5**, the effect caused by the addition of salicylic acid is not only related to the competition between self-protonation and direct protonation, but also, is presumably due to an association step. This reaction would occur between the extra -OH functionality (HD, equations xiii-xix) only present in these two compounds (Scheme 1, highlighted in blue) and the salicylate anion A^-(from *HA*, salicylic acid), and takes place prior to the first electron transfer process. Within this proposed mechanism, the H atom from the extra -OH function (designated as (HD)) acts as the proton source for an intermolecular hydrogen bonding with A^- (equation xiii).

The mechanism is depicted by the following chemical equations upon the consideration that HA is in pre-equilibrium with the species A^- and H^+:

$$(HD)QH + A^- \rightarrow A^-\bullet\bullet\bullet(HD)QH \qquad K_1 \qquad \text{(xiii)}$$

$$A^-\bullet\bullet\bullet(HD)QH + e^- \rightarrow A^-\bullet\bullet\bullet(HD)QH^{\bullet -} \qquad \text{(xiv)}$$

$$A^-\bullet\bullet\bullet(HD)QH^{\bullet -} + H^+ \rightarrow A^-\bullet\bullet\bullet(HD)QH_2^{\bullet} \qquad K_P \qquad \text{(xv)}$$

$$A^-\bullet\bullet\bullet(HD)QH_2^{\bullet} + A^-\bullet\bullet\bullet(HD)QH^{\bullet -} \rightarrow A^-\bullet\bullet\bullet(HD)QH_2^{-} + A^-\bullet\bullet\bullet(HD)QH \qquad \text{(xvi)}$$

$$\text{or } A^-\bullet\bullet\bullet(HD)QH_2^{\bullet} + e^- \rightarrow A^-\bullet\bullet\bullet(HD)QH_2^{-} \qquad \text{(xvii)}$$

$$A^-\bullet\bullet\bullet(HD)QH_2^{-} + H^+ \rightarrow A^-\bullet\bullet\bullet(HD)QH_3 \qquad \text{(xviii)}$$

J. Mex. Chem. Soc. **2025**, *69*(1)
Special Issue

ISSN-e 2594-0317

Hence, the overall reaction mechanism is:

$$A^{-}\bullet\bullet\bullet(HD)QH + 2e^{-} + 2H^{+} \rightarrow A^{-}\bullet\bullet\bullet(HD)QH_3 \qquad \text{(xix)}$$

where $(HD)QH$ and $A^{-}\bullet\bullet\bullet(DH)QH$ represent both non-reduced quinones **4** and **5**, and the complexes being formed between the salicylate ion (A^{-}) and the OH moiety (HD) from the above-mentioned compounds (equation xiii), prior to proton-coupled electron transfer processes.

To calculate an approximate value of (K_1/K_P) from equations xiii and xv, voltammetric simulations were performed following equations i-xix. As previously depicted by Amatore and co-workers when describing reactivity in organic systems, [31] variations in peak potential values (Epc from signal I''c) were analyzed upon varying the kinetic parameter $\lambda = \log (K_1/K_P)C$, where C represents the concentration of the salicylate ion A^{-}. It should be noticed that the increases of salicylate anion are expected to be proportional to the concentration of added salicylic acid, if the acid behaves as a levelled one in DMSO, which is in turn complemented by the two-electron wave shown in Fig. 3. Fig. 4 presents variations of both Epc and i from peak I''c.

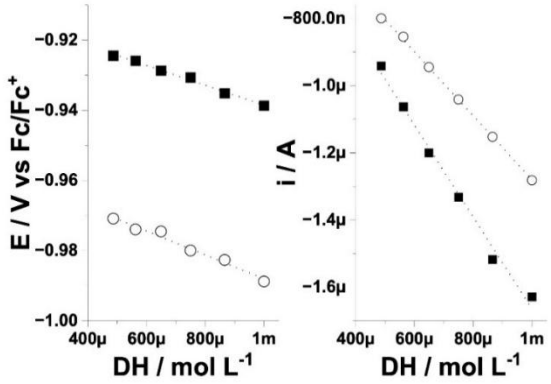

Fig. 4. Variations of potential (E) and current (i) values from I''c peak as a function of the concentration of the salicylate anion A^{-} for *horminone* (■) and *7α-O-methyl-conacytone* (○).

Results showed that the estimated K_1 values for compounds **4** and **5** are 4.7 and 4.5 mol L^{-1} s^{-1}, (Fig. 5) respectively. This mechanism is clearly differentiated from the behaviour observed for **1-3**, namely, a mechanistic transition between two successive electron processes to a bielectronic process, characteristic of a two-electron two-proton transfer.

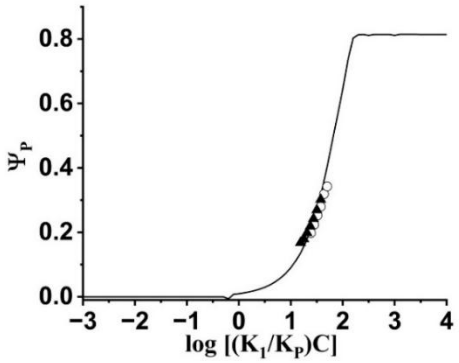

Fig. 5. Working curve of the current function Ψ_P log (K_1/K_P)C, for *horminone* (○) and *7-α-methyl-conacytone* (▲), along with the theoretical simulated curve, where C is the concentration of the salicylate anion A^{-} .

J. Mex. Chem. Soc. **2025**, *69*(1)
Special Issue

ISSN-e 2594-0317

Descriptors to address reactivity of natural abietane α-OHs

To consider the influence of the molecular structures in the experimental results for compounds **4** and **5**, further analysis was required. A strategy based on employing reactivity indexes from quantum chemical calculations to describe the substituent effects during proton-coupled electron transfer processes was employed. Within the [32–35] DFT framework, the reactivity of a system is described by quantum-chemical descriptors, such as those derived from the variations of the electron density (ρ). [36] On this basis, two concepts arise: the chemical potential (μ) and the chemical hardness (η) which are defined as the first and second derivatives of the energy, E[ρ], with respect to the number of electrons, N, at a constant external potential υ(**r**): [37,38]

$$\mu^{\pm} = \left(\frac{\partial E}{\partial N}\right)^{\pm}_{\upsilon(r)} \tag{xx}$$

$$\eta^{\pm} = \left(\frac{\partial^2 E}{\partial N}\right)^{\pm}_{\upsilon(r)} = \left(\frac{\partial^2 \mu}{\partial N}\right)^{\pm}_{\upsilon(r)} \tag{xxi}$$

where the sign of μ and η is indicative of the electron flow, i.e. positive for electron uptake and vice versa. Parr presented an extension of this approach by relating μ and η into a single property by defining the electrophilicity index ω as:

$$\omega = \frac{\mu^2}{2\eta} \tag{xxii}$$

For calculating this index, variations of the energy change (ΔE) for a system in which electron transfer is taking place must be carefully analyzed. Hence, a second-order Taylor expansion of the energy change with the number of electrons gives the following expression: [36]

$$\Delta E = \mu \Delta N + \frac{\Delta N^2}{2} \tag{xxiii}$$

Using the finite differences approximation for μ and η, along with the quadratic equation presented in (xxiii), these quantities are expressed by:[36]

$$\mu = -\frac{I + A}{2} \tag{xxiv}$$

$$\eta = I - A \tag{xxv}$$

where *I* and *A* are the vertical ionization potential and the electron affinity, respectively, and ω becomes approximately

$$\omega \approx \frac{(I + A)^2}{8(I - A)} \tag{xxvi}$$

Electrophilicity-derived global and local reactivity descriptors for addressing the nucleophilic and electrophilic character of a given molecule are expressed as electroaccepting (ω^-) and electrodonating (ω^+) and powers, respectively,[39]

J. Mex. Chem. Soc. **2025**, *69*(1)
Special Issue

ISSN-e 2594-0317

$$\omega^{-} \approx \frac{(3I + A)^2}{16\,(I - A)} \qquad \text{(xxvii)}$$

$$\omega^{+} \approx \frac{(I + 3A)^2}{16\,(I - A)} \qquad \text{(xxviii)}$$

As described by Gázquez, [39] a small value of ω^- implies a larger capability to donate electrons, whereas a large ω^+ value involves an enhanced capability of accepting electrons.

These electrophilicity-related indexes have been successfully related to ETCHB processes; an electron-rich molecule (i.e. semiquinone) can be associated with the electrophilic hydrogen bond donor, DH; therefore, there should be a direct relationship between the binding constant (Table 2) and the electrodonating power. Therefore, ω^+ will be used in this work for explaining the reactivity for the quinone radical anions towards the likely formation of an intermolecular hydrogen bonding, and hence, promoting the formation of the species $A^{-}\bullet\bullet\bullet(DH)QH$ prior to the first electron uptake. For this purpose, after obtaining minimum energy structures, vertical ionization potentials and vertical electron affinities of the species involved in the association step, namely, the radical anions of the quinone compounds were calculated, and results are presented on Table 2. Although not considered for this analysis, calculated properties for compounds 1-3 are included as Supporting Information for this work.

Table 2. Calculated vertical ionization Potentials (I), vertical electron affinities (A), electroaccepting powers ω^+ for the compounds **4** and 5.

	Calculated property (eV)		
Compound	**I**	**A**	**ω^+**
4	6.7828	3.0140	4.1531
5	6.7518	2.9058	3.8887

Although global reactivity indexes serve as a reference for obtaining information on the behaviour of a chemical species as a whole, local reactivity criteria were selected for addressing how changes in electroaccepting capacity modify, on a local scale $\omega^+(\boldsymbol{r})$, the charge transfer ability of the studied radical anions. $\omega^+(\boldsymbol{r})$ is defined as: [39]

$$\omega^+(r) = \frac{(\mu^+)^2}{2\eta^+} f^+\left[\rho_{N_0}; \boldsymbol{r}\right] = \omega^+ f^+\left[\rho_{N_0}; \boldsymbol{r}\right] \qquad \text{(xxvix)}$$

where $f^+\left[\rho_{N_0}; \boldsymbol{r}\right]$ is the condensed-to-atom Fukui function[40] prescribed for nucleophilic attack[41] or charge acceptance,[42] which is related to the differential change in electron density due to an infinitesimal change in the number of electrons, in this case, for an electron acceptance process. For a system of N electrons in a finite-difference approximation, the condensed Fukui function f^+ for all atoms i is given by[40,43]

$$f^+\left[\rho_{N_0}; \boldsymbol{r}\right] = f_i^+ = q_i(N+1) - q_i(N) \qquad \text{(xxx)}$$

where $q_i(N+1)$ and $q_i(N)$ are the charges for the corresponding *N+1* and *N*-electron systems for all atoms *i*. As in previous publications,[42,44] these values were approximated from a Hirshfeld population analysis (Table

J. Mex. Chem. Soc. **2025**, *69*(1)
Special Issue

ISSN-e 2594-0317

3). For this purpose, only the values associated to the -OH moiety were used, since this region is where the formation of the $A^{-}\bullet\bullet\bullet(HD)QH$ complex takes place prior to the semiquinone generation (equation xiii).

Table 3. Calculated charges from Hirshfeld population analysis for *N*+1 and *N* electron structures and local electroaccepting powers $\omega^{+}(\boldsymbol{r})$ for compounds **4** and **5**.

	Calculated property (eV)		
Compound	$\sum_{k} \boldsymbol{q_i(N+1)}$	$\sum_{i} \boldsymbol{q_i(N)}$	$\sum_{i} \boldsymbol{\omega_i}^{+}\boldsymbol{(r)}$
4	-0.1094	-0.1305	0.0877
5	-0.0542	-0.0613	0.0278

It is noteworthy that since **4** has a larger $\omega^{+}(\boldsymbol{r})$ value, and it is therefore expected that this region possesses an enhanced capacity to accept electrons[45] when compared to **5**; however, experimental results showed that they both presented a similar K_1 value. Even though this result is inconclusive for describing the specific values for K1/Kp ratio, it should be noticed that $\omega^{+}(\boldsymbol{r})$ for both compounds is positive, which suggest that the site being considered effectively acts as a hydrogen bonding site. However, further analysis is required, such as electrostatic potential functions as well as experimental variations such as ^{1}H NMR could provide more insights on the influence of this proton in the observed experimental behavior.

Conclusions

An electrochemical study on a series of natural α-hydroxyquinone moieties in abietane diterpenoids (α-OHs) by incorporating increasing concentrations of salicylic acid in the reaction media (AH) was performed. Results showed that binding constants (K) for *horminone* (**4**) and *7α-O-methyl-conacytone* (**5**) were 4.7 and 4.5 M^{-1}, respectively, upon interaction with salicylate anions added during external salicylic acid additions. It is noteworthy that for the rest of the α-OHs under study, a transition from 2/3 electron to a bielectronic (two electron, two proton electron transfer) process took place. While the radical anions generated from the latter compounds are influenced by a self-protonation reaction -due to the acidity of an OH group at C-2 position-, the OH group at nearby sites for **4** and **5** was proved to be a charge-accepting site (nearby the quinone carbonyl function for compound **4** and in the abietanic group for compound **5**). Hence, this specific region is where the intermolecular hydrogen bonding between the hydroxyquinone and the salicylate anion (A^{-}) takes place, presumably generating$A^{-}\bullet\bullet\bullet(DH)QH$ complex prior to electron transfer. This proposed interaction was evaluated by calculating the local electroaccepting power of the involved hydroxyl funcions. These results contribute to the understanding of electrochemical reactivity of abietane compounds for further pharmacological applications.

Acknowledgments

C. Frontana thanks CONAHCYT for support though project A1-S-55204 from Fondo de Investigación Científica Básica 2017-2018. G. Armendáriz-Vidales thanks CONAHCYT for financial support from Estancias Postdoctorales por México 2022(1) Program.

J. Mex. Chem. Soc. **2025**, *69*(1)
Special Issue

ISSN-e 2594-0317

References

1. Thomson, R. in: *Naturally Occurring Quinones*; Elsevier, **2012**.
2. Thomson, R. H. *Pharm Weekbl.* **1991**, *13*, 70–73.
3. Kristensen, S. B.; van Mourik, T.; Pedersen, T. B.; Sørensen, J. L.; Muff, J. *Sci. Rep.* **2020** *10*, 1–10. DOI: https://doi.org/10.1038/s41598-020-70522-z.
4. Gutiérrez-Fernández, J.; Kaszuba, K.; Minhas, G. S.; Baradaran, R.; Tambalo, M.; Gallagher, D. T.; Sazanov, L. A. *Nat. Commun.* **2020**, *11*, 1–17. DOI: https://doi.org/10.1038/s41467-020-17957-0.
5. Diogo, E. B. T.; Dias, G. G.; Rodrigues, B. L.; Guimarães, T. T.; Valença, W. O.; Camara, C. A.; De Oliveira, R. N.; Da Silva, M. G.; Ferreira, V. F.; De Paiva, Y. G.; Goulart, M. O. F.; Menna-Barreto, R. F. S.; De Castro, S. L.; Da Silva Júnior, E. N. *Bioorg. Med. Chem.* **2013**, *21*, 6337–6348. DOI: https://doi.org/10.1016/J.BMC.2013.08.055.
6. O'Brien, P. J. *Chem. Biol. Interact.* **1991**, *80*, 1–41. DOI: https://doi.org/https://doi.org/10.1016/0009-2797(91)90029-7.
7. Silva, T. L.; de Azevedo, M. de L. S. G.; Ferreira, F. R.; Santos, D. C.; Amatore, C.; Goulart, M. O. F. *Curr. Opin Electrochem.* **2020**, *24*, 79–87. DOI: https://doi.org/https://doi.org/10.1016/j.coelec.2020.06.011.
8. Ferreira, F. D. R.; Ferreira, S. B.; Araújo, A. J.; Marinho Filho, J. D. B.; Pessoa, C.; Moraes, M. O.; Costa-Lotufo, L. V.; Montenegro, R. C.; Da Silva, F. D. C.; Ferreira, V. F.; Da Costa, J. G.; De Abreu, F. C.; Goulart, M. O. F. *Electrochim. Acta*. **2013**, *110*, 634–640. DOI: https://doi.org/10.1016/J.ELECTACTA.2013.04.148.
9. Aguilar-Martinez, M.; Macías-Ruvalcaba, N. A.; Bautista-Martínez, J. A.; Gómez, M.; González, F. J.; González, I. *Curr. Org. Chem.* **2004**, *8*, 1721–1738.
10. Ferraz, P. A. L.; De Abreu, F. C.; Pinto, A. V.; Glezer, V.; Tonholo, J.; Goulart, M. O. F. *J. Electroanal. Chem.* **2001**, *507*, 275–286. DOI: https://doi.org/10.1016/S0022-0728(01)00439-9.
11. Abreu, F. C. de; Ferraz, P. A. de L.; Goulart, M. O. F. *J. Braz. Chem. Soc.* **2002**, *13*, 19–35. DOI: https://doi.org/10.1590/S0103-50532002000100004.
12. Shi, R. R. S.; Tessensohn, M. E.; Lauw, S. J. L.; Foo, N. A. B. Y.; Webster, R. D. *Chem. Commun.***2019**, *55*, 2277–2280. DOI: https://doi.org/10.1039/C8CC09188A.
13. Diane K. Smith. *The Chemical Record.* **2021**, *21*, 2488–2501.
14. Gritzner, G.; Kůta, J. *Electrochim. Acta*. **1984**, *29*, 869–873. DOI: https://doi.org/https://doi.org/10.1016/0013-4686(84)80027-4.
15. Aguilar-Martinez, M.; Macias-Ruvalcaba, N. A.; Bautista-Martinez, J. A.; Gomez, M.; Gonzalez, F. J.; Gonzalez, I. *Curr. Org. Chem.* **2005**, *8*, 1721–1738. DOI: https://doi.org/10.2174/1385272043369548.
16. Costentin, C. E. *Chem. Rev.* **2008**, *108*, 2145–2179. DOI: https://doi.org/10.1021/cr068065t.
17. Amatore, C.; Capobianco, G.; Farnia, G.; Sandona, G.; Saveant, J. M.; Severin, M. G.; Vianello, E. *J. Am. Chem. Soc.* **1985**, *107*, 1815–1824. DOI: https://doi.org/10.1021/ja00293a003.
18. Kupchan, S. M.; Karim, A.; Marcks, C. *J. Org. Chem.* **1969**, *34*, 3912–3918.
19. Frontana, C.; Frontana-Uribe, B. A.; González, I. *Electrochim. Acta*. **2003**, *48*, 3593–3598. DOI: https://doi.org/10.1016/S0013-4686(03)00479-1.
20. Frontana, C.; González, I. *J. Electroanal. Chem.* **2007**, *603*, 155–165. DOI: https://doi.org/10.1016/J.JELECHEM.2007.01.024.
21. Maldonado, T.; Martínez-González, E.; Frontana, C. *Electroanalysis.* **2016**, *28*, 2827–2833. DOI: https://doi.org/10.1002/ELAN.201600255.
22. Armendáriz-Vidales, G.; Martínez-González, E.; Cuevas-Fernández, H. J.; Fernández-Campos, D. O.; Burgos-Castillo, R. C.; Frontana, C. *Electrochim. Acta*. **2013**, *110*, 628–633. DOI: https://doi.org/10.1016/j.electacta.2013.05.123.

J. Mex. Chem. Soc. **2025**, *69*(1)
Special Issue

ISSN-e 2594-0317

23. Gómez, M.; González, F. J.; González, I. *Electroanalysis*. **2003**, *15*, 635–645. DOI: https://doi.org/10.1002/ELAN.200390080.
24. Gómez, M.; González, F. J.; González, I. *J. Electroanal. Chem.* **2005**, *578*, 193–202. DOI: https://doi.org/10.1016/j.jelechem.2004.12.036.
25. Nadjo, L.; Savéant, J. M. *J. Electroanal. Chem. Interfacial Electrochem.* **1973**, *48*, 113–145. DOI: https://doi.org/https://doi.org/10.1016/S0022-0728(73)80300-6.
26. Schenck, G.; Baj, K.; Iggo, J. A.; Wallace, M. *Anal. Chem.* **2022**, *94*, 8115–8119. DOI: https://doi.org/10.1021/ACS.ANALCHEM.2C00200/ASSET/IMAGES/LARGE/AC2C00200_0001.JPEG.
27. Amatore, C.; Capobianco, G.; Farnia, G.; Sandona, G.; Saveant, J. M.; Severin, M. G.; Vianello, E. *J. Am. Chem. Soc*. **1985**, *107*, 1815–1824.
28. Armendáriz-Vidales, G.; Hernández-Muñoz, L. S.; González, F. J.; de Souza, A. A.; de Abreu, F. C.; Jardim, G. A. M.; da Silva, E. N. Jr.; Goulart, M. O. F.; Frontana, C. *J. Org. Chem.* **2014**, *79*, 5201–5208. DOI: https://doi.org/10.1021/jo500787q.
29. Martínez-González, E.; Armendáriz-Vidales, G.; Ascenso, J. R.; Marcos, P. M.; Frontana, C. *J. Org. Chem*. **2015**, *80*, 4581–4589. DOI: https://doi.org/10.1021/acs.joc.5b00441.
30. Martínez-González, E.; Frontana, C. *J. Org. Chem.* **2014**, *79*, 1131–1137. DOI: https://doi.org/10.1021/jo402565t.
31. Armendáriz-Vidales, G.; Frontana, C. *Org. Biomol. Chem.* **2014**, *12*, 6393–6398. DOI: https://doi.org/10.1039/C4OB01207K.
32. Parr, R. G.; Szentpály, L. v.; Liu, S. *J. Am. Chem. Soc.* **1999**, *121*, 1922–1924. DOI: https://doi.org/10.1021/ja983494x.
33. Parr, R. G.; Pearson, R. G. *J. Am. Chem. Soc.* **1983**, *105*, 7512–7516. DOI: https://doi.org/10.1021/ja00364a005.
34. Parr, R. G.; Donnelly, R. A.; Levy, M.; Palke, W. E. *J. Chem. Phys.* **1978**, *68*, 3801–3807. DOI: https://doi.org/10.1063/1.436185.
35. Gázquez, J. L.; Cedillo, A.; Vela, A. *J. Phys. Chem. A.* **2007**, *111*, 1966–1970. DOI: https://doi.org/10.1021/jp065459f.
36. Contreras, R. R.; Fuentealba, P.; Galván, M.; Pérez, P. *Chem. Phys. Lett.* **1999**, *304*, 405–413. DOI: https://doi.org/https://doi.org/10.1016/S0009-2614(99)00325-5.
37. Pal, R.; Chattaraj, P. K. *J. Comput. Chem.* **2023**, *44*, 278–297. DOI: https://doi.org/10.1002/JCC.26886.
38. Martínez-González, E.; Armendáriz-Vidales, G.; Ascenso, J. R.; Marcos, P. M.; Frontana, C. *J. Org. Chem.* **2015**, *80*, 4581–4589. DOI: https://doi.org/10.1021/ACS.JOC.5B00441/SUPPL_FILE/JO5B00441_SI_001.PDF.
39. Yang, W.; Mortier, W. J. *J. Am. Chem. Soc.* **1986**, *108*, 5708–5711. DOI: https://doi.org/10.1021/JA00279A008.
40. Martínez-González, E.; Frontana, C. *J. Org. Chem.* **2014**, *79*, 1131–1137. DOI: https://doi.org/10.1021/JO402565T/SUPPL_FILE/JO402565T_SI_001.PDF.
41. Gázquez, J. L. *J. Mex. Chem. Soc*. **2008**, *52*, 3–10. DOI: https://doi.org/10.29356/jmcs.v52i1.1040.